

Article

Distribution of the Deposition Rates in an Industrial-Size PECVD Reactor Using HMDSO Precursor

Žiga Gosar^{1,2}, Denis Donlagić³, Simon Pevec³ , Bojan Gergič³, Miran Mozetič^{4,5} , Gregor Primc^{4,5} , Alenka Vesel^{4,5,*}  and Rok Zaplotnik^{4,5} 

¹ Development and Technology Department, Elvez Ltd, Ulica Antona Tomšiča 35, 1294 Višnja Gora, Slovenia; ziga.gosar@elvez.si

² Ecotechnology Programme, Jozef Stefan International Postgraduate School, Jamova Cesta 39, 1000 Ljubljana, Slovenia

³ Faculty of Electrical Engineering and Computer Science, University of Maribor, Koroška Cesta 46, 2000 Maribor, Slovenia; denis.donlagic@um.si (D.D.); simon.pevec@um.si (S.P.); bojan.gergic@um.si (B.G.)

⁴ Department of Surface Engineering, Jozef Stefan Institute, Jamova Cesta 39, 1000 Ljubljana, Slovenia; miran.mozetic@ijs.si (M.M.); gregor.primc@ijs.si (G.P.); rok.zaplotnik@ijs.si (R.Z.)

⁵ Research and Development Department, Plasmadis Ltd., Teslova Ulica 30, 1000 Ljubljana, Slovenia

* Correspondence: alenka.vesel@guest.arnes.si

Abstract: The deposition rates of protective coatings resembling polydimethylsiloxane (PDMS) were measured with numerous sensors placed at different positions on the walls of a plasma-enhanced chemical vapor deposition (PECVD) reactor with a volume of approximately 5 m³. The plasma was maintained by an asymmetric capacitively coupled radiofrequency (RF) discharge using a generator with a frequency 40 kHz and an adjustable power of up to 8 kW. Hexamethyldisiloxane (HMDSO) was leaked into the reactor at 130 sccm with continuous pumping using roots pumps with a nominal pumping speed of 8800 m³ h⁻¹ backed by rotary pumps with a nominal pumping speed of 1260 m³ h⁻¹. Deposition rates were measured versus the discharge power in an empty reactor and a reactor loaded with samples. The highest deposition rate of approximately 15 nm min⁻¹ was observed in an empty reactor close to the powered electrodes and the lowest of approximately 1 nm min⁻¹ was observed close to the precursor inlet. The deposition rate was about an order of magnitude lower if the reactor was fully loaded with the samples, and the ratio between deposition rates in an empty reactor and loaded reactor was the largest far from the powered electrodes. The results were explained by the loss of plasma radicals on the surfaces of the materials facing the plasma and by the peculiarities of the gas-phase reactions typical for asymmetric RF discharges.

Keywords: HMDSO; PECVD; deposition rate; uniformity of deposition; polymerization; organosilicon thin films



Citation: Gosar, Ž.; Donlagić, D.; Pevec, S.; Gergič, B.; Mozetič, M.; Primc, G.; Vesel, A.; Zaplotnik, R. Distribution of the Deposition Rates in an Industrial-Size PECVD Reactor Using HMDSO Precursor. *Coatings* **2021**, *11*, 1218. <https://doi.org/10.3390/coatings11101218>

Academic Editors: Alessio Lamperti and Alessandro Patelli

Received: 26 August 2021

Accepted: 30 September 2021

Published: 5 October 2021

Publisher's Note: MDPI stays neutral with regard to jurisdictional claims in published maps and institutional affiliations.



Copyright: © 2021 by the authors. Licensee MDPI, Basel, Switzerland. This article is an open access article distributed under the terms and conditions of the Creative Commons Attribution (CC BY) license (<https://creativecommons.org/licenses/by/4.0/>).

1. Introduction

Many materials should be coated with a thin protective layer to provide an adequate surface finish and stability in harsh environments [1–5]. A variety of techniques have been proposed, and a few have also been commercialized [6–10]. One technique for depositing compact and hydrophobic films similar to polydimethylsiloxane (PDMS) is plasma polymerization. A suitable monomer is provided and partially dissociated and ionized under plasma conditions [11,12]. The radicals adhere to the surface of any object exposed to the plasma and form a thin film. The structure and composition of the coating depend on the type of precursor, plasma parameters and specifics of the discharge used for sustaining gaseous plasma [13–17]. The growth kinetics is complex and difficult to control because of the large number of radicals formed in the gaseous plasma. An early report of the kinetics was presented by Bourreau et al. [18]. The authors used different sources to deposit protective coatings rich in silicon oxides: silane (SiH₄), hexamethyl disiloxane (HMDSO) and tetraethoxysilane (TEOS). They correlated the evolution of the coverage

with the deposition kinetics and compared the growth rates. The profiles were independent of the substrate temperature or the deposition rate when silane was used as a precursor. In the case of organic precursors, however, the deposition rate decreased with an increase in the deposition temperature. They found the adsorption–desorption phenomena to be important factors for the coverage evolution. At low deposition temperatures, the film growth rate was sensitive to ion surface bombardment and resulted in a non-conformal deposit even in compounds with high surface mobility.

Theirich et al. [19] studied the gas-phase reactions in HMDSO/O₂ mixtures and pressures between 20 and 70 Pa. Plasma was characterized by mass spectrometry and infrared spectroscopy. They found the film homogeneity dominated by the precursor content and its spatial distribution in the gas or plasma phase. Three reactive intermediate species were proposed to act as a precursor for silica-like film growth, all having a mass of 148 Da, so the authors concluded that further work should be performed to distinguish between the radicals.

In their classic paper, Hegemann et al. [20] studied the deposition rate and three-dimensional uniformity of capacitively coupled radio-frequency (RF) plasma useful for depositing protective layers using HMDSO as a precursor. The deposition rate increased with monomer gas flow, whereas it was independent of pressure. Large differences in the deposition rates at different positions of the samples were reported, as well as the influence of the dimensions of the samples on the growth kinetics. In another paper [21], the same group investigated the deposition rate in symmetrical and asymmetrical electrode configurations and found that the deposition rate depended on the so-called reaction parameter (power input per gas flow of the monomer).

More recently, Ropcke's [22] group performed a detailed characterization of the HMDSO plasma by optical emission spectroscopy (OES) in the visible spectral range and infrared laser absorption spectroscopy (IRLAS). They used a plasma reactor of a rather large power density (discharge power per volume of the discharge chamber) of the order of 100 W per liter. They managed to derive the concentrations of the various stable and unstable plasma species, which were found to be in the range between 10¹⁷ and 10²¹ m⁻³. They also studied the influence of the discharge parameters, such as power, pressure and gas mixture, on the molecular concentrations. Based on the construction principle of the reactor, the plasma generation was characterized by a certain degree of inhomogeneity with different temperature zones, i.e., hottest, hot and colder zones. This complexity was characterized by the multiple molecular species, including the HMDSO precursor and products in the ground and excited states existing in the plasma.

Plasma-enhanced chemical vapor deposition (PECVD) technique for the deposition of protective coatings from HMDSO was commercialized decades ago despite the experimentally observed non-homogeneities and instabilities, which may lead to inadequate properties of the deposited films. Recently, Gosar et al. [16] reported that the composition of the deposited films depended on the time-evolution of the plasma parameters, although the discharge parameters (power, pressure, flow rate, pumping speed) remained fairly constant. The time evolution was explained by the drifting plasma parameters, which was detrimental to the quality of the protective films, especially where a rather high power density was used to sustain the gaseous plasma. At low discharge powers, however, the properties of the deposited films were not time dependent. The quality of the films is a crucial parameter in the industrial application of the PECVD technique using HMDSO, so many industrial reactors operate at a very low power density to minimize the risk [23]. On the other hand, the low power density results in a poor deposition rate, as explained by the above-cited authors.

The problem of plasma non-uniformity and the resultant deviations of the film thickness from the desired value in large plasma reactors may be suppressed by rotating samples upon plasma processing [24]. This is a standard solution in commercial reactors for depositing protective coatings in batch mode. The samples are mounted on planetaria and moved through zones with different plasma parameters. The relatively long treatment time

(several minutes in commercial plasma reactors) ensures a reasonable coating thickness and uniformity. Still, the problem arising from plasma inhomogeneities is not solved, so there is a need to develop configurations of plasma reactors with deposition rates that are as uniform as possible throughout the entire reactor.

Commercial reactors for the deposition of the protective coatings using the HMDSO as the precursor may be upgraded if the non-uniformities are known and understood. Several groups have already reported the non-uniformity in plasma parameters, but only a few have measured the deposition rates in different parts of the plasma reactor [12,13,20]. The present paper provides measurements of the deposition rate performed with several sensors mounted in selected positions within a large plasma reactor. The deposition rates for an empty and a fully loaded reactor were measured to reveal the influence of the samples on the non-uniformity of the deposition rates.

2. Materials and Methods

2.1. Plasma-Enhanced Chemical Vapor Deposition Reactor

The industrial PECVD reactor useful for the deposition of PDMSO-like coatings was presented in detail in our previous paper [25]. The reactor has a cylindrical shape with a diameter of 1.9 m and a height of 1.8 m. During the deposition, the reactor was pumped with two roots pumps with a total nominal pumping speed $8800 \text{ m}^3 \text{ h}^{-1}$, backed by two rotary pumps of a total nominal pumping speed $1260 \text{ m}^3 \text{ h}^{-1}$. Before the deposition, in order to get the base pressure as low as possible (around 0.02 Pa), the reactor was also pumped with two diffusion pumps with a total pumping speed $35,000 \text{ L/s}$. HMDSO was the only gas that was introduced into the plasma reactor. It was introduced through a calibrated flow controller. The pressure was measured with a Pirani gauge. At the HMDSO inlet of 130 sccm ($\text{cm}^3/\text{min}_{\text{STP}}$), which is the standard flow rate used in mass production, the pressure was about 4 Pa . Plasma was characterized by optical emission spectroscopy (OES) AvaSpec-Mini4096CL (Avantes, Apeldoorn, Netherlands) near one of the powered electrodes as shown in Figure 1.

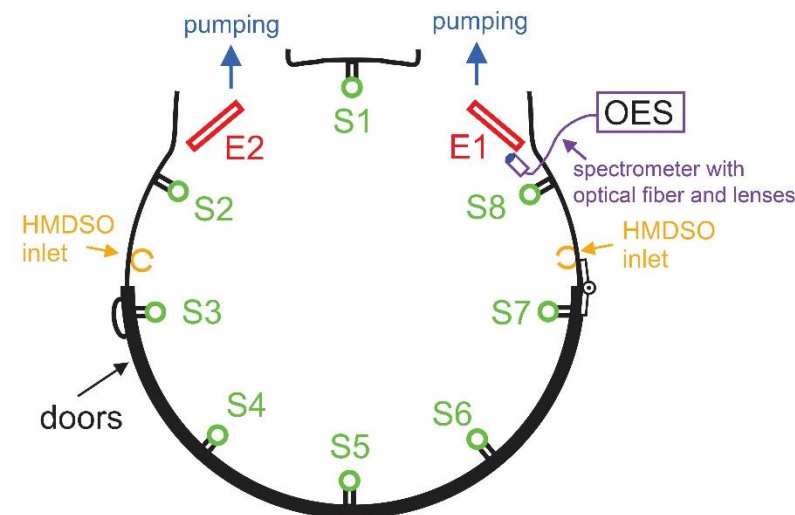


Figure 1. Cross-section of the cylindrical PECVD reactor with the position of the pump ducts, powered electrodes (E1, E2), HMDSO inlet, sensors for deposition rate measurements (S1–S8), OES lens, optical fiber and OES spectrometer.

An asymmetric capacitively coupled RF discharge was used for sustaining gaseous plasma. The discharge was powered by an RF generator (PE II 10K, Advanced Energy, Denver, CO, USA) operating at 40 kHz and adjustable power between 1 and 8 kW . A couple of powered electrodes were mounted close to the pump duct. The area of each electrode was approximately 0.4 m^2 . The area of the grounded electrode (housing) was approximately 16 m^2 . The ratio between the areas of the powered and grounded electrodes was

approximately 40. Therefore, the plasma was sustained by an asymmetrical capacitive coupled RF discharge, and the gradients in the plasma parameters were expected.

The HMDSO inlet was provided through vertically oriented grounded metallic tubes, as shown in Figure 1. The tubes were positioned close to the grounded walls of the plasma reactor. They had small holes separated by 15 cm. The precursor was thus introduced into the reactor unevenly.

2.2. Sensors of the Deposition Rate

Eight sensors were fixed on the sidewalls of the plasma reactor (BDS-MF, Arzuffi, Vallezio Bellini, Italy) for the real-time monitoring of the deposition rate, as shown in Figure 1 (marked with S1 to S8). The sensor S1 was positioned on the rough grid, which separates the discharge chamber from the polycold pump duct, which was not used in this experiment. A photo of the sensor S1 is shown in Figure 2a. Other sensors were fixed on the chamber walls on the grounded housing.

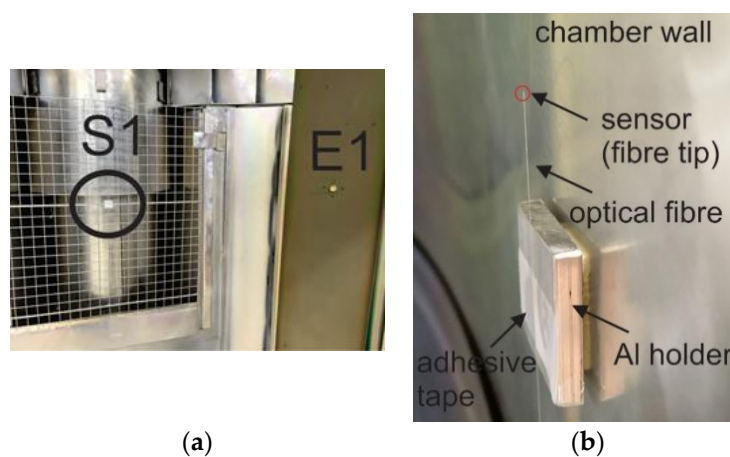


Figure 2. (a) Fixation of the sensor S1 and (b) the photo of a sensor mounting.

Each sensor essentially consisted of a single-mode optical fiber, which was cleaved and exposed to the processing chamber on one side, while being connected to an appropriate opto-electronics signal integration system on the other side. Opto-electronics signal integration system launched light into the fiber, while acquiring and processing back-reflected optical power from cleaved fiber end. Since the deposited PDMSO-like layer has a different refractive index than vitreous silica, the back-reflectance from the cleaved fiber end changed during the PDMSO deposition. This change was correlated with the change in thickness of the deposited material. The correlation was obtained by an appropriate calibration and processing of acquired signals. One such sensor was already used in our previous work [26], where the deposition rates measured with such sensor in real time were the same as those measured with time-consuming post-deposition surface analysis such as atomic force microscopy (AFM) (Solver PRO, NT-MDT, Moscow, Russia), X-ray photoelectron spectroscopy (XPS) (TFA XPS Physical Electronics, München, Germany) and time-of-flight secondary ion mass spectrometry (ToF-SIMS) depth profiles (ToF-SIMS 5 instrument, ION-TOF GmbH, Münster, Germany).

Figure 2b shows a photo of an optical fiber sensor fixed on the aluminum holder, which was fixed on the wall of the plasma reactor.

2.3. Optical Emission Spectroscopy (OES)

An optical lens was mounted in the PECVD reactor (Figure 1) and connected with optical fiber through optical feedthrough to a standard low-resolution optical spectrometer Avantes AvaSpec-Mini4096CL (Avantes, Apeldoorn, Netherlands). The spectrometer measures light emission spectra. The device is based on AvaBench 75 symmetrical Czerny Turner design with a 4096-pixel CCD detector with a focal length of 75 mm. The range

of measurable wavelengths is from 200 nm to 1100 nm, and the wavelength resolution is 0.5 nm. The spectrometer has a USB2.0 interface, enabling high sampling rates up to 150 spectra per second. Signal-to-noise ratio is 300:1. Integration time is adjustable from 30 μ s to 50 s. At integration times below 6.5 ms, the spectrometer itself performs internal averaging of spectra before transmitting them through the USB interface. The spectrometer was connected to the process computer via USB. The integration time was set to 5 s.

3. Results and Discussion

Plasma in the empty discharge chamber was characterized by OES. Here it should be stressed that an empty chamber means that there are no samples and no planetaria (sample holders) inside the reactor. A typical OES spectrum is shown in Figure 3. The spectrum consists of Balmer series of radiative transitions of H atoms from excited states to the first excited state. The next prominent spectral feature arises from the relaxation of the CH radicals with the bandhead at 431 nm. Other features are marginal. The OES indicates partial dissociation of the precursor molecules, but otherwise, it does not provide any additional significant information. Other radicals are also in the reactor, but their emission is marginal. More interesting is the intensity of the spectral features versus the discharge power. Figure 4 shows quite linear curves. The emission intensity depends on the electron density and temperature as well as the density of radicals in the ground state, and the dependence is not trivial. Still, the behavior of the lines in Figure 4 indicates either more extensive dissociation of the precursor molecules or higher electron density/temperature or both at higher power. This observation is expected, considering that the optical lens for acquiring spectra was mounted just next to the powered electrode.

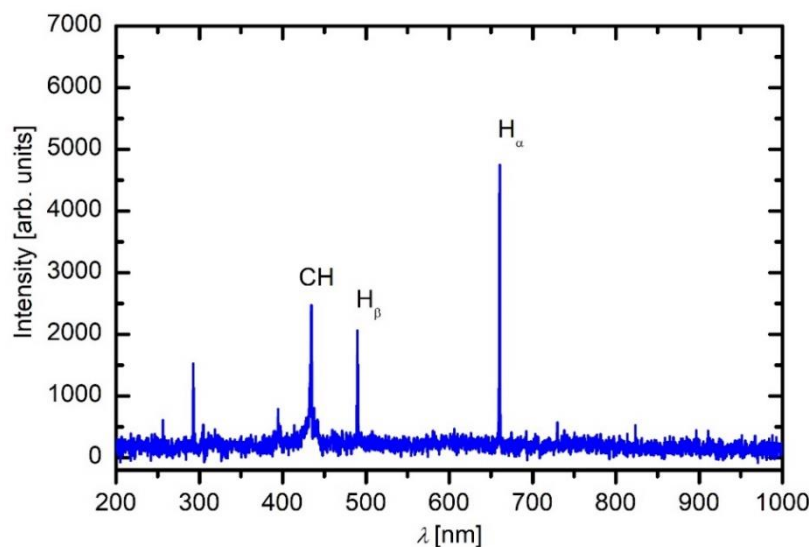


Figure 3. An optical spectrum of the plasma at the discharge power of 5 kW and 130 sccm of HMDSO.

Figure 5 shows the measured deposition rate versus the discharge power. Interestingly enough, the deposition rate is rather constant in the broad range of powers from approximately 2 to 7 kW. This observation is not correlated with data in Figure 4, which shows a gradual increase in the emission intensity. This paradox can be explained by a fact already reported for small experimental systems [16]: only moderate dissociation of the precursor is sufficient for a reasonable deposition rate. Extensive dissociation of the precursor leads to the formation of various radicals that do not stick to the sample surface but are pumped out from the system; therefore, in cases where large power densities are used for sustaining plasma in HMDSO, the deposit does not resemble PDMS but rather silica. Detailed study of the transition from polymer-like films to films rich in silicon oxides was reported in [16]. The power density used in this study was at least 10 times lower than

the power density needed for such full transition; however, there are still mild transitions, towards films richer in silicon, that can affect the deposition rates seen in Figure 5.

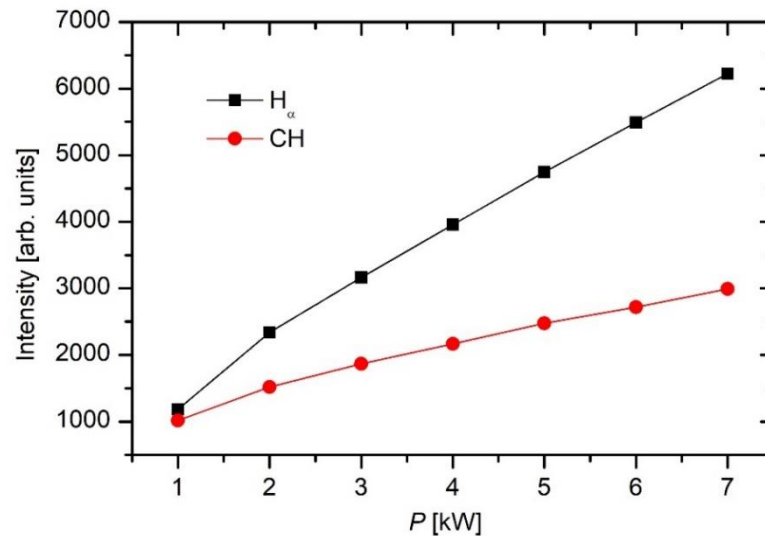


Figure 4. The intensity of the H_α and CH lines at 656 nm and 431 nm as a function of the discharge power at 130 sccm HMDSO.

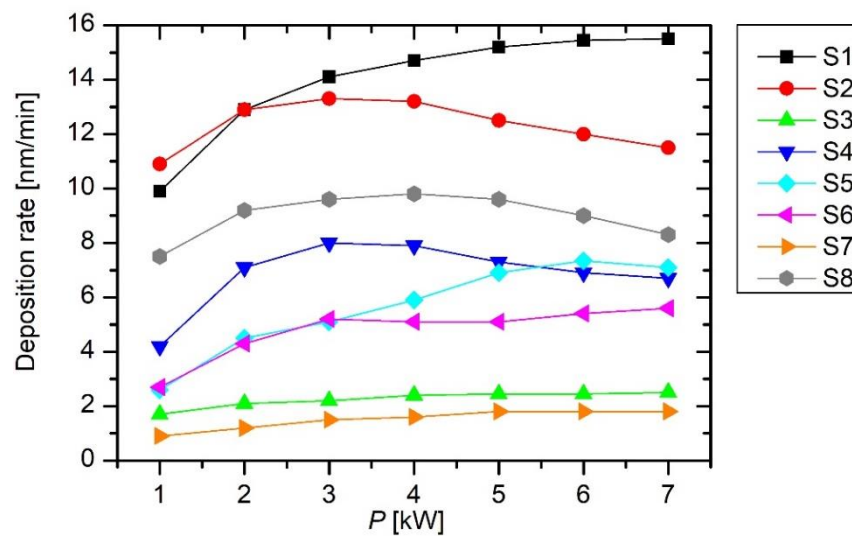


Figure 5. The deposition rate versus the discharge power in the empty reactor.

Both Figures 5 and 6 indicate large differences in the deposition rate at different locations ranging from 1.6 to 14.7 nm min⁻¹. The deposition rate is the largest for sensor S1. This sensor was placed on the grid between the electrodes, as shown in Figures 1 and 2. The highest deposition rate is on the surface, where it is not needed because the radicals at the position of S1 are likely to be pumped away from the system. The high deposition rate indicates a high density of radicals that are capable of forming the protective coating. According to the state-of-the-art, such radicals are partially dissociated HMDSO molecules, including those found at the mass of 148 Da [19]. In the empty chamber, these radicals are denser or more concentrated at the position near the pump ducts than anywhere else in the system, as revealed in Figures 5 and 6.

Figure 6 shows the thickness of the coating obtained from the sensors' signals versus the treatment time for the empty plasma reactor. One can observe almost perfectly linear behavior, which indicates excellent stability of plasma parameters during the deposition of the protective coatings. The stability may be a consequence of the appropriately low

pressure in the reactor, which prohibits instabilities that may appear because of the cluster formation [27] and thus the loss of radicals useful for the deposition of the protective coating.

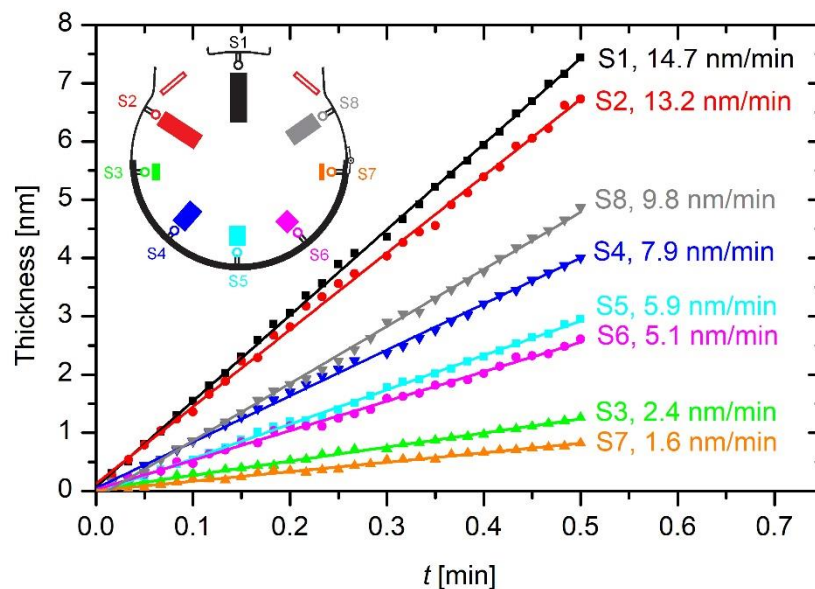


Figure 6. The thickness of the deposited films derived from the sensors' signals (points) with linear fits (lines) versus the plasma treatment time in an empty reactor at a power of 4 kW at 130 sccm HMDSO. In the inset figure, a deposition rate is presented with the height of the column at a sensor position.

Examining Figure 5 and compared to Figure 1, one observes the next largest deposition rate at sensors S2 and S8, which were located a bit farther from the pump ducts. In fact, sensors S2 and S8 were located between the gas inlet and the powered electrodes, as shown in Figure 1. The possible reasons for favored deposition rate at these positions will be discussed later in this report.

The deposition rates at the position of sensors far from the electrodes are lower but still reasonably high. For example, Figure 5 reveals the deposition rates of about 6 nm min^{-1} for the sensors S4, S5, and S6. Conversely, sensors S3 and S7, which were placed close to the gas inlet but away from the powered electrodes, show a poor deposition of approximately 2 nm min^{-1} .

The distribution of the deposition rate in the plasma reactor provides a qualitative model of the gas kinetics that allows the most reasonable degree of fragmentation of the precursor molecules. The injected HMDSO molecules do not interact with the solid materials but should be partially dissociated to radicals with a reasonable sticking coefficient. The plasma density far from the powered electrodes in the reactor used for these experiments is only on the order of 10^{14} m^{-3} [23]. Such a low density of electrons does not enable immediate dissociation to useful fragments. This may explain the poor deposition rates detected by sensors S3 and S7, located close to the gas inlet but away from the powered electrodes. The molecules should be allowed a prolonged residence time in the weakly ionized gaseous plasma to dissociate into useful radicals. The residence time will be estimated later in this paper. The injected precursor molecules enter the plasma reactor with a significant drift velocity but quickly thermalize (assume the random motion after a few elastic collisions). The motion is then governed by diffusion, i.e., it is random. The molecules suffer numerous collisions with plasma electrons while diffusing from the source (gas inlet) to the position of the sensors S4, S5, and S6. The gas at the position of these sensors is thus reasonably well dissociated, which favors the deposition on the surfaces far away from the electrodes. As mentioned above, the residence time of the

injected molecules is too short to cause significant deposition at the positions of sensors S3 and S7.

Sensors S2 and S8 are as close to the gas inlet as S3 and S7, but Figure 5 indicates a deposition rate several times higher at S2 and S8 compared to S3 or S7. This paradox may be explained by the larger residence time of molecules striking the surface of the sensors at positions S2 and S8, but the variation of the plasma density versus the distance from the powered electrode may be more important. The asymmetric capacitively coupled RF discharge is characterized by an oscillating sheath next to the powered electrode. Since the frequency of these oscillations is rather low (the RF generator operates at 40 kHz), the electrons oscillate within the sheath and gain energy enough for a rather extensive dissociation and ionization of the gaseous molecules within the oscillating sheath [28]. Therefore, the dissociation of the precursor molecules is more extensive next to the electrodes than in the bulk plasma far away from the powered electrodes. As a result, the deposition rate at the sensors S2 and S8 is favorable despite the proximity of the gas inlet.

The radicals stick to surfaces of any material facing plasma; therefore, the deposition rate as determined by the sensors located in the reactor according to Figure 1 should be lower if the reactor is additionally loaded with samples. To study the influence of samples on the deposition rate, samples were mounted on the planetaria, as shown in Figure 7. About 250 medium-sized, approximately 40-cm-long samples, which represented about 100% of the total chamber capacity, were evenly distributed inside the chamber. The height and the diameter of the planetaria were 160 cm and 55 cm, respectively, and the distance between axles was around 60 cm. The planetaria were spinning at a speed of 6 rpm. The deposition rate measurements were repeated with sensors located at the same positions as in the empty chamber. The results are shown in Figure 8. The highest deposition rate was observed for the sensors S2 and S8. These sensors are located between the gas inlet and the powered electrode (Figure 1). The deposition rate at the positions S2 and S8 are about an order of magnitude greater than at any other position except near the pump ducts. The presence of samples in the plasma reactor, therefore, influences the deposition rate significantly. Not only is it lower than in the empty reactor (compare Figures 6 and 9), but a reasonably large deposition rate is observed only in the region close to the electrodes (S2, S8, and S1). Elsewhere, the deposition rate is below 1 nm min^{-1} .



Figure 7. A photo of the fully loaded chamber with samples mounted on planetaria.

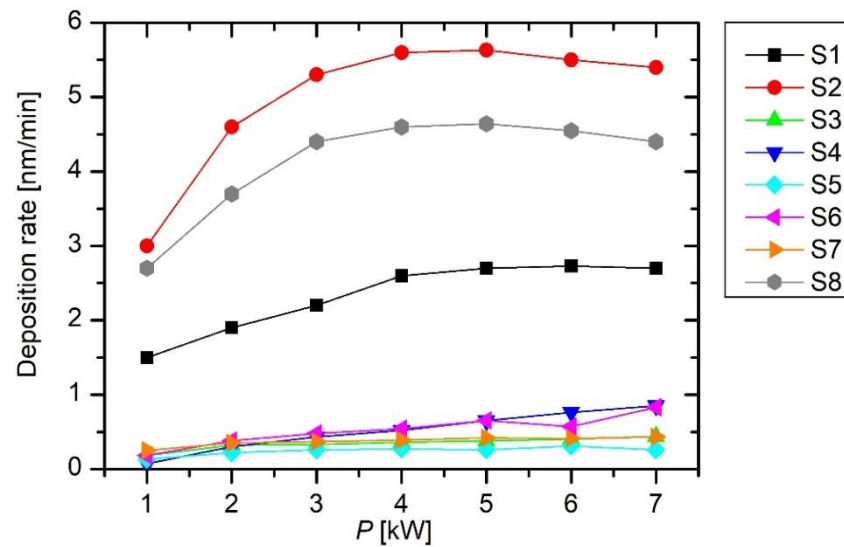


Figure 8. The deposition rate versus the discharge power in reactor loaded with samples.

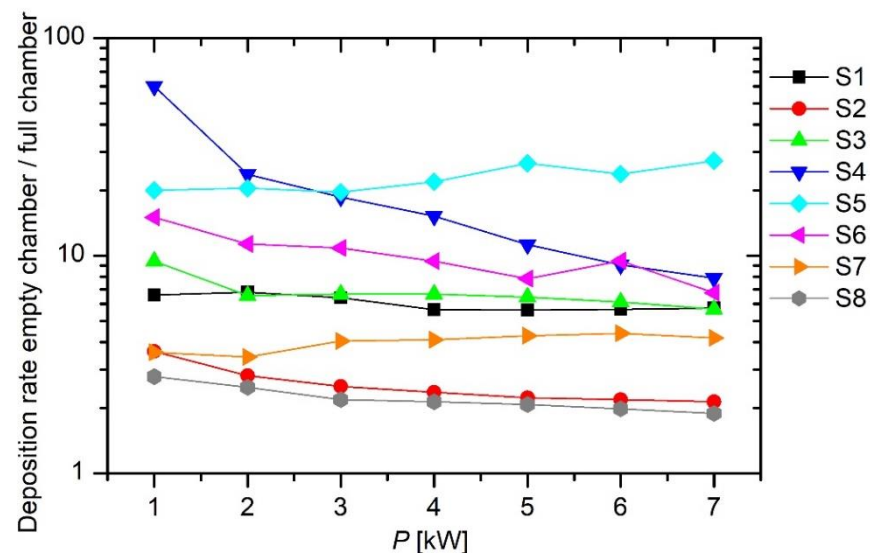


Figure 9. The deposition rate versus the discharge power in reactor loaded with samples.

The very low deposition rate at S4, S5, and S6, as observed in Figure 8, is explained by the loss of radicals on the surfaces of the samples. As discussed above, the plasma density away from the electrodes is low, so the loss of radicals useful for depositing protective coating cannot be balanced by production because of electron-impact dissociation. Conversely, the deposition rate close to the powered electrode (sensors S2 and S8) remains reasonably high because of the higher electron energy in the oscillating sheath.

The ratio between the deposition rate in an empty reactor and a full reactor is shown in Figure 9. The highest ratio of 10–20 is observed for sensors positioned far from the electrodes. This observation was already explained by the loss of radicals on the surface of the samples. However, the ratio is much lower for the sensors positioned close to the powered electrodes. For sensors S2 and S8, the ratio is approximately 3 for the lowest power of 1 kW and only 2 for the highest power of 7 kW. The power-dependence of the ratio is explained by the fact that the electron energy in the vicinity of the powered electrodes is much higher than far from the electrodes, so a significant fraction of injected HMDSO molecules get dissociated and thus contribute to the film growth.

The upper discussion reveals the crucial role of the residence time of molecules in the plasma reactor. Gaseous molecules diffuse in the plasma reactor because the random

velocity is much higher than the drifting from the gas inlet to the pump ducts. The drift velocity of gaseous molecules at the entrance to the pump ducts can be calculated if the effective pumping speed at that position is known. The effective pumping speed depends on the nominal pumping speed of the roots pumps and the conductivity of any vacuum elements mounted between the roots pumps and the plasma reactor. The conductivity is difficult to determine, but one can also determine the effective pumping speed from the measured gas flow and pressure inside the reactor by considering the constant mass flow:

$$p_1 S_1 = p_2 S_2. \quad (1)$$

Here, p_1 is the atmospheric pressure, S_1 is the gas flow as measured by the flow controller, p_2 is the measured pressure in the plasma reactor, and S_2 is the effective pumping speed at the grid which separates the plasma reactor and the pump ducts. Taking into account the measured values, i.e., $p_1 = 10^5$ Pa, $S_1 = 130$ cm³/min = 2×10^{-6} m³ s⁻¹, $p_2 = 4$ Pa, one can estimate the effective pumping speed as:

$$S_2 = p_1 S_1 / p_2 = 0.05 \text{ m}^3 \text{ s}^{-1} = 180 \text{ m}^3 \text{ h}^{-1}. \quad (2)$$

As calculated from Equation (1), the effective pumping speed is an order of magnitude lower than the nominal pumping speed of the roots pumps. This observation may be explained by the deviation of the real pumping speed of the roots pumps from the nominal value (the latter is just the maximum pumping speed at optimal conditions) and the limited conductivity of vacuum elements mounted between the plasma reactor and the roots pumps.

There is a negligible pressure gradient throughout the plasma reactor, because the conductivity is orders of magnitude greater than the effective pumping speed. The cross-section of the plasma reactor is a product of the reactor diameter and height, i.e., $A = 3.5$ m². The gas drift velocity from the source to the pump ducts is:

$$v = S_2 / A = 0.014 \text{ m s}^{-1}. \quad (3)$$

This value is orders of magnitude lower than the random velocity due to the thermal motion of the molecules, which is:

$$\bar{v} = \sqrt{\frac{8kT}{\pi m}} = 200 \text{ m s}^{-1}. \quad (4)$$

In Equation (4), we considered the room temperature ($T = 300$ K) and the HMDSO mass $m = 162$ Da. By considering the distance between the gas inlet and the grid separating the reactor from the pump ducts of $l = 1$ m, one can estimate the average residence time of gaseous molecules as:

$$\tau = l / v = 80 \text{ s}. \quad (5)$$

The residence time as calculated from Equation (5) is an averaged value taking into consideration the simple calculations. Because the random velocity as calculated from Equation (4) is orders of magnitude higher than the drift velocity as determined from Equation (3), the residence time is spread broadly from the value calculated using Equation (5), and thus it should be taken just as an estimation. In any case, the residence time is long enough to assure for numerous collisions with plasma electrons. The large residence time is the reason for the rather large deposition rate at any position far from the gas inlet in the empty reactor. The maximal deposition is observed on the grid near the pump ducts (sensor S1) in the empty reactor. The radicals entering the pump ducts are likely to have been created well before reaching the grid.

Plasma reactors are useful only when the coatings are deposited on various products mounted on the planetaria. Technologically relevant results are presented in Figure 8. The deposition rate at sensor S1 (mounted on the grid near the pump ducts) is moderate at

about 2 nm min^{-1} , which is favorable from the technological point of view. Still, a significant fraction of the radicals useful for the thin film deposition is pumped out from the reactor. However, the major deficiency of the plasma reactor is the poor deposition rate at any other position. Despite the long residence time of gaseous radicals, the deposition rate is poor because of the loss of radicals on the samples placed on the planetaria. The only useful part of the reactor, when loaded with samples, is at positions S2 and S8, so close to the powered electrodes. The discharge configuration in this reactor is, therefore, inadequate. The configuration with electrodes placed opposite to the pump duct should be better.

No sensor was placed on a powered electrode because it would heat significantly. Still, according to the measured deposition rates and according to the above discussion, it is reasonable to assume the large deposition rate on the powered electrodes. In fact, the electrodes should occasionally be etched in chemical baths to remove the excessive deposits. The extensive deposition of thin films on the electrodes and thus loss of radicals for coating the samples is a major drawback of the reactor used in this study. The problem could be minimized using symmetric discharge, but it is often not feasible as in our PECVD reactor.

Despite the large dissipation of the deposition rate, the composition of the deposited films remains similar for all films at the positions of different sensors. Figure 10 represents the composition of the films as deduced from XPS survey spectra. The measurements were performed in the reactor loaded with samples. The concentration of carbon is close to 50 at.%, while the concentrations of oxygen and silicon is between 25 and 30 at.% for all samples. The small variations in the composition may be attributed to the accuracy of the XPS technique or to actual variation in the composition, but because the differences are marginal it is possible to conclude that the stoichiometry of the deposited films does not vary significantly between different positions in the plasma reactor.

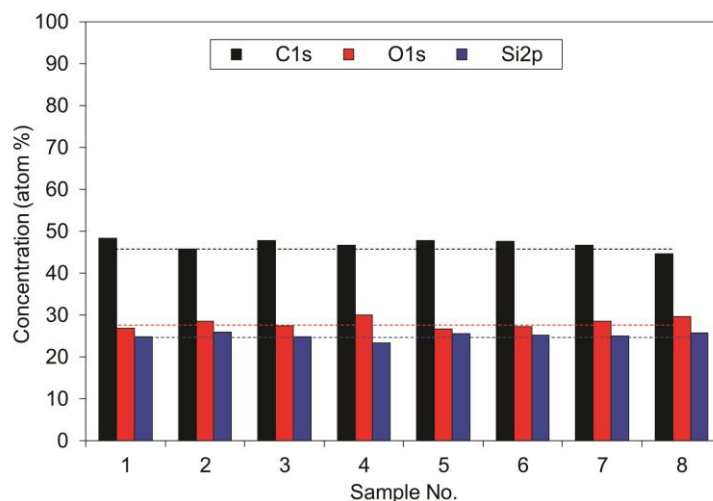


Figure 10. Concentrations of carbon, oxygen and silicon of deposited films at different positions in the PECVD reactor as deduced from XPS survey spectra.

4. Conclusions

Many commercial plasma reactors for the deposition of thin films from organic precursors using the PECVD technique suffer from non-uniform deposition rates. Moving the products to be coated by placing them on planetaria enables reasonable coating uniformity, but the efficiency is poor, because a significant fraction of the precursor radicals used as building blocks of the protective coatings are lost by adsorption on the powered electrodes and/or by pumping out from the reactor. An attempt was made to measure the deposition rates at various locations inside an industrial reactor powered by a capacitively coupled RF discharge. The plasma reactor had a volume of approximately 5 m^3 . The maximum deposition rate for an empty reactor was measured on a grid near the pump ducts. The next

highest rates were measured close to the powered electrodes, but a reasonable deposition rate was also observed far from the powered electrodes or the pump duct. The observation was interpreted by the formation of radicals useful for the deposition of the thin films throughout the reactor. The average residence time of approximately 80 s ensured a reasonably large production rate, despite the very low electron density in the plasma away from the oscillating sheaths next to the powered electrodes. Loading the reactor with numerous samples caused a significant difference in the deposition rates. Not only were they lower, but the distribution changed significantly. The deposition rates far from the powered electrodes dropped by more than an order of magnitude for a fully loaded chamber. Deposition rates above about 1 nm min^{-1} were only observed close to the powered electrodes. These observations indicate the need for modification of the discharge configuration in the industrial plasma reactor for depositing protective coatings from HMDSO precursor using the PECVD technique.

Author Contributions: Conceptualization, R.Z., D.Đ. and S.P.; methodology, R.Z., Ž.G. and D.Đ.; software, G.P. and D.Đ.; validation, D.Đ., B.G. and A.V.; formal analysis, A.V., Ž.G. and B.G.; investigation, R.Z., G.P. and Ž.G.; resources, Ž.G. and D.Đ.; data curation, M.M., S.P. and B.G.; writing—original draft preparation, M.M.; writing—review and editing, A.V.; supervision, M.M.; project administration, G.P.; funding acquisition, D.Đ. and M.M; All authors have read and agreed to the published version of the manuscript.

Funding: This research was funded by the Slovenian Research Agency, grant number L2-1835 (Innovative sensors for real-time monitoring of deposition rates in plasma-enhanced chemical vapor deposition (PECVD) systems) and research core funding grant number P2-0082 (Thin-film structures and plasma surface engineering).

Institutional Review Board Statement: Not applicable.

Informed Consent Statement: Not applicable.

Data Availability Statement: Not applicable.

Conflicts of Interest: The authors declare no conflict of interest.

References

1. Kotte, L.; Althues, H.; Mäder, G.; Roch, J.; Kaskel, S.; Dani, I.; Mertens, T.; Gammel, F.J. Atmospheric pressure PECVD based on a linearly extended DC arc for adhesion promotion applications. *Surf. Coat. Technol.* **2013**, *234*, 8–13. [[CrossRef](#)]
2. Schwarz, J.; Schmidt, M.; Ohl, A. Synthesis of plasma-polymerized hexamethyldisiloxane (HMDSO) films by microwave discharge. *Surf. Coat. Technol.* **1998**, *98*, 859–864. [[CrossRef](#)]
3. Morent, R.; de Geyter, N.; van Vlierberghe, S.; Dubruel, P.; Leys, C.; Schacht, E. Organic–inorganic behaviour of HMDSO films plasma-polymerized at atmospheric pressure. *Surf. Coat. Technol.* **2009**, *203*, 1366–1372. [[CrossRef](#)]
4. Choudhury, A.J.; Barve, S.A.; Chutia, J.; Pal, A.R.; Kishore, R.; Pande, M.; Patil, D.S. RF-PACVD of water repellent and protective HMDSO coatings on bell metal surfaces: Correlation between discharge parameters and film properties. *Appl. Surf. Sci.* **2011**, *257*, 8469–8477. [[CrossRef](#)]
5. Benítez, F.; Martínez, E.; Esteve, J. Improvement of hardness in plasma polymerized hexamethyldisiloxane coatings by silica-like surface modification. *Thin Solid Film.* **2000**, *377–378*, 109–114. [[CrossRef](#)]
6. Huang, J.; Cai, Y.; Xue, C.; Ge, J.; Zhao, H.; Yu, S.-H. Highly stretchable, soft and sticky PDMS elastomer by solvothermal polymerization process. *Nano Res.* **2021**. [[CrossRef](#)]
7. Mohania, V.; Deshpande, T.D.; Singh, Y.R.G.; Patil, S.; Mangal, R.; Sharma, A. Fabrication and characterization of porous poly(dimethylsiloxane) (PDMS) adhesives. *ACS Appl. Polym. Mater.* **2021**, *3*, 130–140. [[CrossRef](#)]
8. Pezzana, L.; Riccucci, G.; Spriano, S.; Battagazzore, D.; Sangermano, M.; Chiappone, A. 3D printing of PDMS-like polymer nanocomposites with enhanced thermal conductivity: Boron nitride based photocuring system. *Nanomaterials* **2021**, *11*, 373. [[CrossRef](#)] [[PubMed](#)]
9. Schäfer, J.; Foest, R.; Quade, A.; Ohl, A.; Weltmann, K.D. Local deposition of SiO_x plasma polymer films by a miniaturized atmospheric pressure plasma jet (APPJ). *J. Phys. D Appl. Phys.* **2008**, *41*, 194010. [[CrossRef](#)]
10. Belmonte, T.; Henrion, G.; Gries, T. Nonequilibrium atmospheric plasma deposition. *J. Therm. Spray Technol.* **2011**, *20*, 744. [[CrossRef](#)]
11. Hamedani, Y.; Macha, P.; Bunning, T.J.; Naik, R.R.; Vasudev, M.C. Chemical Vapor Deposition - Recent Advances and Applications in Optical, Solar Cells and Solid State Devices. In *Plasma-Enhanced Chemical Vapor Deposition: Where we are and the Outlook for the Future*; Neralla, S., Ed.; IntechOpen: Rijeka, Croatia, 2016.

12. Hegemann, D.; Bülbül, E.; Hanselmann, B.; Schütz, U.; Amberg, M.; Gaiser, S. Plasma polymerization of hexamethyldisiloxane: Revisited. *Plasma Processes and Polymers*. **2021**, *18*, 2000176. [[CrossRef](#)]
13. Top, M.; Schönfeld, S.; Fahlteich, J.; Bunk, S.; Kühnel, T.; Straach, S.; De Hosson, J.T. Hollow-cathode activated PECVD for the high-rate deposition of permeation barrier films. *Surf. Coat. Technol.* **2017**, *314*, 155–159. [[CrossRef](#)]
14. Trunec, D.; Navrátil, Z.; Stahel, P.; Zají Ková, L.; Bur Íková, V.; Cech, J. Deposition of thin organosilicon polymer films in atmospheric pressure glow discharge. *J. Phys. D Appl. Phys.* **2004**, *37*, 2112–2120. [[CrossRef](#)]
15. Zajíčková, L.; Buršíková, V.; Kučerová, Z.; Franta, D.; Dvořák, P.; Šmíd, R.; Peřina, V.; Macková, A. Deposition of protective coatings in rf organosilicon discharges. *Plasma Sources Sci. Technol.* **2007**, *16*, S123–S132. [[CrossRef](#)]
16. Gosar, Ž.; Kovač, J.; Đonlagić, D.; Pevec, S.; Primc, G.; Junkar, I.; Vesel, A.; Zaplotnik, R. PECVD of hexamethyldisiloxane coatings using extremely asymmetric capacitive RF discharge. *Materials* **2020**, *13*, 2147. [[CrossRef](#)]
17. Hnilica, J.; Schäfer, J.; Foest, R.; Zajíčková, L.; Kudrle, V. PECVD of nanostructured SiO₂ in a modulated microwave plasma jet at atmospheric pressure. *J. Phys. D Appl. Phys.* **2013**, *46*, 335202. [[CrossRef](#)]
18. Bourreau, C.; Catherine, Y.; Garcia, P. Growth kinetics and step coverage in plasma deposition of silicon dioxide from organosilicon compounds. *Mat. Sci. Eng. A*. **1991**, *139*, 376–379. [[CrossRef](#)]
19. Theirich, D.; Soll, C.; Leu, F.; Engemann, J. Intermediate gas phase precursors during plasma CVD of HMDSO. *Vacuum* **2003**, *71*, 349–359. [[CrossRef](#)]
20. Hegemann, D.; Brunner, H.; Oehr, C. Deposition rate and three-dimensional uniformity of RF plasma deposited SiO_x films. *Surf. Coat. Technol.* **2001**, *142–144*, 849–855. [[CrossRef](#)]
21. Hegemann, D.; Brunner, H.; Oehr, C. Evaluation of deposition conditions to design plasma coatings like SiO_x and a-C:H on polymers. *Surf. Coat. Technol.* **2003**, *174–175*, 253–260. [[CrossRef](#)]
22. Nave, A.S.C.; Mitschker, F.; Awakowicz, P.; Röpcke, J. Spectroscopic studies of microwave plasmas containing hexamethyldisiloxane. *J. Phys. D Appl. Phys.* **2016**, *49*, 395206. [[CrossRef](#)]
23. Gosar, Ž.; Kovač, J.; Mozetič, M.; Primc, G.; Vesel, A.; Zaplotnik, R. Characterization of gaseous plasma sustained in mixtures of HMDSO and O₂ in an industrial-scale reactor. *Plasma Chem. Plasma Process.* **2020**, *40*, 25–42. [[CrossRef](#)]
24. Wang, B.; Fu, X.; Song, S.; Chu, H.O.; Gibson, D.; Li, C.; Shi, Y.; Wu, Z. Simulation and optimization of film thickness uniformity in physical vapor deposition. *Coatings* **2018**, *8*, 325. [[CrossRef](#)]
25. Gosar, Ž.; Kovač, J.; Mozetič, M.; Primc, G.; Vesel, A.; Zaplotnik, R. Deposition of SiO_xC_yH_z protective coatings on polymer substrates in an industrial-scale PECVD reactor. *Coatings* **2019**, *9*, 234. [[CrossRef](#)]
26. Gosar, Ž.; Đonlagić, D.; Pevec, S.; Kovač, J.; Mozetič, M.; Primc, G.; Vesel, A.; Zaplotnik, R. Deposition kinetics of thin silica-like coatings in a large plasma reactor. *Materials* **2019**, *12*, 3238. [[CrossRef](#)] [[PubMed](#)]
27. Despax, B.; Gaboriau, F.; Caquineau, H.; Makasheva, K. Influence of the temporal variations of plasma composition on the cyclic formation of dust in hexamethyldisiloxane-argon radiofrequency discharges: Analysis by time-resolved mass spectrometry. *Aip Adv.* **2016**, *6*, 105111. [[CrossRef](#)]
28. Chabert, P.; Tsankov, T.V.; Czarnetzki, U. Foundations of capacitive and inductive radio-frequency discharges. *Plasma Sources Sci. Technol.* **2021**, *30*, 024001. [[CrossRef](#)]